

UAV Attitude, Heading, and Wind Estimation Using GPS/INS and an Air Data System

Matthew Rhudy^{*}, Trenton Larrabee[†], Haiyang Chao[‡], Yu Gu[§], and Marcello R. Napolitano^{**}
Department of Mechanical and Aerospace Engineering, West Virginia University, Morgantown, WV, 26506

A new attitude, heading, and wind estimation algorithm is proposed, which incorporates measurements from an air data system to properly relate predicted attitude information with aircraft velocity information. Experimental Unmanned Aerial Vehicle (UAV) flight data was used to validate the proposed approach. The experimental results demonstrated effective estimation of the roll, pitch, yaw, and heading angles, and provided a smoothed estimate of the angle of attack and sideslip angles. The wind estimation results were validated with respect to measurements provided by a local weather station. It was shown that this new method of attitude estimation is effective in distinguishing the yaw and heading angles of the aircraft, properly regulating the attitude estimates with air data system measurements, and providing a reasonable estimate of the local wind field.

Nomenclature

a_x, a_y, a_z	=	acceleration in aircraft body frame (m/s ²)
\mathbf{b}	=	bias parameter vector
\mathbf{f}	=	state prediction function
g	=	acceleration due to gravity (m/s ²)
\mathbf{h}	=	observation function
k	=	discrete time index
l	=	power law exponent
p	=	roll rate (deg/s)
\mathbf{Q}	=	process noise covariance matrix
q	=	pitch rate (deg/s)
\mathbf{R}	=	measurement noise covariance matrix
r	=	yaw rate (deg/s)
T_s	=	sampling time (s)
u, v, w	=	body-axis velocity components (m/s)
\mathbf{u}	=	input vector
\mathbf{v}	=	measurement noise vector
V	=	total airspeed (m/s)
V_{pitot}	=	Pitot tube airspeed (m/s)
V_x, V_y, V_z	=	Earth-fixed components of velocity (m/s)
W	=	random walk coefficient
w_x, w_y, w_z	=	wind velocity components (m/s)
\mathbf{w}	=	process noise vector
\mathbf{x}	=	state vector
\mathbf{y}	=	output vector
z	=	height above ground (m)
\mathbf{z}	=	measurement vector

^{*} Ph.D. Candidate, Mechanical and Aerospace Engineering (MAE) Department, PO Box 6106, mbr5002@gmail.com, AIAA Student Member.

[†] M.S. Student, MAE Department, PO Box 6106.

[‡] Postdoctoral Researcher, MAE Department, PO Box 6106, AIAA Member.

[§] Assistant Professor, MAE Department, PO Box 6106, AIAA Senior Member.

^{**} Professor, MAE Department, PO Box 6106, AIAA Senior Member.

α	=	angle of attack (deg)
β	=	sideslip angle (deg)
θ	=	pitch angle (deg)
ϕ	=	roll angle (deg)
ψ	=	yaw angle (deg)

I. Introduction

THE estimation of aircraft states and parameters can be a challenging problem due to the inevitable presence of wind. This difficulty is especially prevalent for small Unmanned Aerial Vehicle (UAV) applications, due to their smaller size and weight. One particular problem of interest is low-cost attitude estimation, which is important for many aircraft applications such as flight control¹ and remote sensing². A popular approach to the attitude estimation problem involves the integration of sensor information from a Global Positioning System (GPS) receiver with that of a low-cost Inertial Navigation System (INS)³. Various formulations of attitude estimation using GPS/INS sensor fusion exist in the literature⁴⁻⁷, containing comparison studies evaluating different algorithms and nonlinear estimators.

A problem with the existing work in GPS/INS sensor fusion for attitude estimation⁴⁻⁷ is that it implicitly assumes that the angle of attack and sideslip angles of the aircraft are zero, i.e. the aircraft is always pointing in the direction of its total velocity. The INS can be used to predict the attitude angles of the aircraft effectively through time integration of the rate gyroscope measurements from an Inertial Measurement Unit (IMU). Since these estimates tend to drift with time due to sensor biases, GPS velocity measurements are then used to regulate this drifting phenomenon. However, when using GPS velocity to regulate the attitude angles, current work implicitly makes a simplifying assumption that the orientation of the aircraft is equivalent to the direction of the total velocity of the aircraft. While under many operating conditions this approximation can lead to reasonable results, a more theoretically justifiable formulation should consider air data information in order to properly relate the INS predicted attitude with the GPS velocity calculations. The work presented herein derives a new formulation of attitude estimation that includes measurements from an Air Data System (ADS). The ADS provides measurements of the airspeed, angle of attack, and sideslip angle. The contribution of this work is that it provides a means for accurately estimating the true attitude of the aircraft, allows for a clear distinction between the heading and yaw angles of the aircraft, provides a smoothed estimate of the airspeed, angle of attack, and sideslip, and provides an estimate of the local wind speed and direction.

In this work, the wind field is estimated for both horizontal and vertical wind in order to properly correct INS attitude estimates with GPS velocity information. These wind estimates, however, can also be used for other purposes. Estimation of the wind field is useful in UAV applications for various objectives such as dropping objects, target tracking, geolocation⁸, automatic control⁹, energy harvesting, trajectory optimization¹⁰, and air traffic control¹¹. There is some existing work in the area of wind estimation, which was used for inspiration in deriving the new attitude and wind estimation formulation. Lefas developed a simple filter for wind estimation using magnetic heading, true airspeed, and radar measurements¹¹. Kumon *et al.* studied the estimation of horizontal wind using a delta wing UAV with an iterative optimization approach, and validated the results with weather data from a meteorological agency⁹. Langelan *et al.* presented a thorough simulation study of a direct method for estimating the wind field¹⁰. Cho *et al.* presented a horizontal wind estimation method using the Extended Kalman Filter (EKF)¹² with both simulated and experimentally collected flight data⁸. The horizontal wind speed and direction were predicted using a random walk noise assumption, then these states were regulated through the wind triangle comparison of ground speed from GPS and air speed⁸. The work presented herein expands upon this concept to include vertical wind, and also incorporates angle of attack and sideslip information, which are useful in relating the aircraft body frame to the wind frame.

The rest of this paper is organized as follows. Section II provides the derivation and description of the new attitude and wind estimation formulation. Section III describes the experimental UAV platform that was used to collect data for this study. Section IV presents some estimation results, followed by a conclusion in Section V.

II. Problem Formulation

This work considers the estimation of aircraft body-axis velocity components (u, v, w), Euler attitude angles, (ϕ, θ, ψ), and three-axis wind velocity components, (w_x, w_y, w_z). This estimation is performed through the fusion of IMU measurements of three-axis accelerations (a_x, a_y, a_z) and angular rates (p, q, r), GPS velocity components (V_x, V_y, V_z), and ADS measurements from a Pitot tube (V_{pitot}) and wind vanes for angle of attack (α) and sideslip (β). Additionally, a bias parameter vector was considered for the inertial sensors which are known to contain biases on

the measurement signal^{4,7}. Using these values, the state space system is formulated with the following state vector, \mathbf{x} , bias parameter vector, \mathbf{b} , input vector, \mathbf{u} , and output vector, \mathbf{y} :

$$\begin{aligned}\mathbf{x} &= [u \quad v \quad w \quad \phi \quad \theta \quad \psi \quad w_x \quad w_y \quad w_z]^T \\ \mathbf{b} &= [b_{a_x} \quad b_{a_y} \quad b_{a_z} \quad b_p \quad b_q \quad b_r]^T \\ \mathbf{u} &= [a_x \quad a_y \quad a_z \quad p \quad q \quad r]^T \\ \mathbf{y} &= [V_x \quad V_y \quad V_z \quad V_{pitot} \quad \alpha \quad \beta]^T\end{aligned}\tag{1}$$

The bias parameters are subtracted from the measured input vector before use in the filter

$$\mathbf{u} = \hat{\mathbf{u}} - \mathbf{b}\tag{2}$$

where $\hat{\mathbf{u}}$ denotes the measured input vector from the IMU.

First, the state dynamics are defined. The conversion between the body-axes and Earth-fixed axes is given by the Direction Cosine Matrix (**DCM**), which is defined by successive rotations of the roll, pitch, and yaw angles (ϕ , θ , ψ) of the aircraft

$$\mathbf{DCM}(\phi, \theta, \psi) = \mathbf{R}_z(\psi) \mathbf{R}_y(\theta) \mathbf{R}_x(\phi)\tag{3}$$

where the rotation matrices are defined as

$$\mathbf{R}_x(\phi) = \begin{bmatrix} 1 & 0 & 0 \\ 0 & \cos \phi & -\sin \phi \\ 0 & \sin \phi & \cos \phi \end{bmatrix}\tag{4}$$

$$\mathbf{R}_y(\theta) = \begin{bmatrix} \cos \theta & 0 & \sin \theta \\ 0 & 1 & 0 \\ -\sin \theta & 0 & \cos \theta \end{bmatrix}\tag{5}$$

$$\mathbf{R}_z(\psi) = \begin{bmatrix} \cos \psi & -\sin \psi & 0 \\ \sin \psi & \cos \psi & 0 \\ 0 & 0 & 1 \end{bmatrix}\tag{6}$$

The state dynamics for the body-axis velocity states are then given by¹³

$$\begin{bmatrix} \dot{u} \\ \dot{v} \\ \dot{w} \end{bmatrix} = \begin{bmatrix} rv - qw + a_x \\ pw - ru + a_y \\ qu - pv + a_z \end{bmatrix} + \mathbf{DCM}(\phi, \theta, \psi)^T \begin{bmatrix} 0 \\ 0 \\ g \end{bmatrix}\tag{7}$$

The attitude state dynamics are defined using¹⁴

$$\begin{bmatrix} \dot{\phi} \\ \dot{\theta} \\ \dot{\psi} \end{bmatrix} = \begin{bmatrix} 1 & \sin \phi \tan \theta & \cos \phi \tan \theta \\ 0 & \cos \phi & -\sin \phi \\ 0 & \sin \phi \sec \theta & \cos \phi \sec \theta \end{bmatrix} \begin{bmatrix} p \\ q \\ r \end{bmatrix}\tag{8}$$

Due to the random nature of wind, e.g. turbulence, it is challenging to predict the future behavior of the local wind field dynamics. Therefore, the wind velocity state dynamics are modeled as a random walk process⁸.

The state dynamic equations have been defined in continuous-time using the following format

$$\dot{\mathbf{x}} = \mathbf{f}_c(\mathbf{x}, \mathbf{u}) \quad (9)$$

where \mathbf{f}_c is the nonlinear continuous-time state transition function. In order to implement these equations in a discrete-time filter, a first order discretization is used¹⁵

$$\mathbf{x}_k = \mathbf{x}_{k-1} + T_s \mathbf{f}_c(\mathbf{x}_{k-1}, \mathbf{u}_{k-1}) + \mathbf{w}_k \triangleq \mathbf{f}(\mathbf{x}_{k-1}, \mathbf{u}_{k-1}) + \mathbf{w}_k \quad (10)$$

where \mathbf{f} is the nonlinear discrete-time state transition function, T_s is the sampling time of the system, and \mathbf{w} is the zero-mean Gaussian process noise vector with covariance matrix, \mathbf{Q} .

To define the dynamics for the bias parameters, a first order Gauss-Markov noise model was used. In a related work¹⁶, the Allan variance¹⁷ approach presented in^{18,19} was used to determine the parameters of the first order Gauss-Markov noise model for the dynamics of the bias on each IMU channel. The Gauss-Markov noise model for each sensor measurement involves two parameters: a time constant and a variance of the wide band sensor noise. Using this model, the dynamics for the bias parameters are given by

$$\mathbf{b}_k = \mathbf{b}_{k-1} e^{-\frac{T_s}{\boldsymbol{\tau}}} + \mathbf{n}_{k-1} \quad (11)$$

where $\boldsymbol{\tau}$ is a vector of time constants and \mathbf{n} is a zero-mean noise vector with variance given by a diagonal matrix of the variance terms for each sensor. The time constant and variance terms were calculated in¹⁶ for each channel of the same IMU that was considered for this study.

Next, the output equations are defined. In order to properly relate the velocity information, the **DCM** is again used to relate the body frame to the Earth-fixed frame. Using this relationship, the body-axis velocity components can be rotated into the Earth-fixed frame and corrected for wind by^{10,13}

$$\begin{bmatrix} V_x \\ V_y \\ V_z \end{bmatrix} = \mathbf{DCM}(\phi, \theta, \psi) \begin{bmatrix} u \\ v \\ w \end{bmatrix} + \begin{bmatrix} w_x \\ w_y \\ w_z \end{bmatrix} \quad (12)$$

The Pitot tube is mounted in the aircraft along the longitudinal axis, therefore it will measure the airspeed in the body x -axis, thus defining the simple output equation

$$V_{pitot} = u \quad (13)$$

The angle of attack and sideslip angle are calculated from the body-axis velocity components using¹³

$$\alpha = \tan^{-1} \left(\frac{w}{u} \right) \quad (14)$$

$$\beta = \sin^{-1} \left(\frac{v}{\sqrt{u^2 + v^2 + w^2}} \right)$$

Using these relationships, the output equations are defined in the following form

$$\mathbf{y}_k = \mathbf{h}(\mathbf{x}_k) + \mathbf{v}_k \quad (15)$$

where \mathbf{h} is the nonlinear observation function and \mathbf{v} is the zero-mean Gaussian measurement noise vector with covariance matrix, \mathbf{R} . The measurement vector, \mathbf{z} , is provided by GPS velocity calculations, Pitot tube airspeed, and wind vane measurements.

In addition to this GPS/INS/ADS sensor fusion formulation, a comparatively tuned GPS/INS formulation is considered, which is equivalent to the GPS/INS/ADS formulation except that the wind states are removed and the ADS measurements are omitted from the measurement update. This formulation is used as a comparison, in order to illustrate the benefits of using the ADS information. Since both the GPS/INS/ADS and GPS/INS sensor fusion formulations contain nonlinear functions, a nonlinear state estimation technique such as the Extended Kalman Filter (EKF)¹² or Unscented Kalman Filter (UKF)²⁰ is required. The UKF was selected for this study due to its ease of implementation (no need to calculate Jacobian matrices)^{21,22}. The equations for the UKF are well documented in various sources, e.g.^{5,23,24}, and therefore are not presented here.

III. Experimental Platform

This study uses flight data collected with the ‘Red Phastball’ small UAV which was designed, manufactured, and instrumented by researchers of the Flight Control Systems Lab (FCSL) at West Virginia University (WVU). The avionic payload includes a custom designed printed circuit board (PCB) featuring four redundant Analog Devices® Inertial Measurement Units (IMUs) and a Novatel OEM-V1 GPS receiver, as shown in Fig. 1.

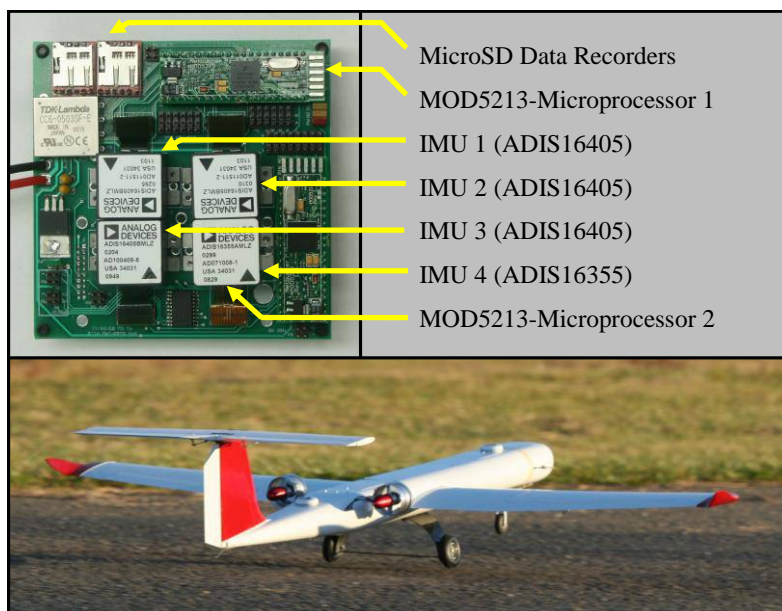


Fig. 1. WVU Red Phastball UAV and Avionics Board

The avionics board records measurements using μ SD data loggers interfaced with the measurement systems using two MOD-5213 microprocessors. Although each IMU has an actual resolution of 14-bit, the resolution is improved by oversampling the signals at 200 Hz, then averaging down to 50 Hz, thus achieving a near equivalent of 18-bit resolution. Note that since typical low-cost attitude estimation uses a single IMU, for this study only the data from one of the IMUs, an Analog Devices ADIS16405, is used. Data were also collected from two angle of attack and one sideslip wind vanes attached to potentiometers with 10 V A/D at 16-bit resolution. A Pitot tube was mounted on the nose of the aircraft along the longitudinal axis, connected to Sensor Technics pressure sensors. The air data measurement system is shown in Fig. 2.



Fig. 2. Air Data Measurement System

For precision time alignment purposes, a Pulse Per Second (PPS) signal from the GPS receiver is recorded with the IMU data using an Analog to Digital (A/D) port on the MOD-5213 microprocessor. The GPS receiver calculates the local position and velocity using GPS satellite information. In addition to IMU and GPS data, a high-quality Goodrich® mechanical vertical gyroscope was used to obtain direct measurements at 50 Hz of the roll and pitch of the aircraft with 3.3 V A/D at 16-bit resolution. These measurements are used as a ‘truth’ reference in order to evaluate the low-cost attitude estimation performance.

To provide some validation data for the wind estimation, a portable ground weather station was installed during the flight test. A Peet Brothers Ultimeter 2100 weather station, shown in Fig. 3, was used to collect wind data at ~3 Hz with an accuracy of 0.9 m/s for the wind speed and 5% for the 16-point magnetic direction sensing. The weather station setup is mounted securely near the flight path at approximately 7 m off the ground.



Fig. 3. Ground Weather Station

The measurements of wind from the weather station and the UAV are taken at different altitudes, both of which are relatively close to the ground. For altitudes of up to ~200 m, the wind profile is approximated using the following power law due to the ground friction effects^{8,25}

$$V_z = V_{ref} \left(\frac{z}{z_{ref}} \right)^l \quad (16)$$

where V_z is the scalar mean wind speed at height z above ground level, V_{ref} is the scalar mean wind speed at reference height z_{ref} , and l is the power law exponent. An existing study indicated the power law exponent of 1/7 to be effective for neutral stability conditions, therefore this value was used²⁶. The power law correction was considered in order to more properly match the wind speed measured by the weather station to the wind speed measured by the UAV. The altitude of the UAV was estimated using the GPS position for this correction.

IV. Results

A set of flight data was collected with the WVU Red Phastball for use in this study. This data set is approximately 5 minutes in duration from takeoff to landing of the aircraft. The flight included lateral and longitudinal doublet maneuvers. Using the sensor data from this flight, estimation results were calculated using both the GPS/INS/ADS and GPS/INS sensor fusion formulations. Due to the availability of the ‘truth’ measurement from the vertical gyroscope, the error in the estimates of the roll and pitch angles can be calculated. Over the entire length of flight, the standard deviation of the roll and pitch errors is given in Table 1. For an illustrative representation of the roll and pitch estimation results, a 20 second segment of the estimated roll and pitch angle with corresponding vertical gyroscope (VG) measurements is shown in Fig. 4. Similar estimation performance is shown for the GPS/INS/ADS and GPS/INS formulations in Table 1 and Fig. 4. However, in order to witness the benefits of the GPS/INS/ADS formulation, the other states are considered.

Table 1. Summary of Roll and Pitch Estimation Performance

	Roll Error Standard Deviation	Pitch Error Standard Deviation
GPS/INS/ADS	1.01 deg	1.31 deg
GPS/INS	1.03 deg	1.19 deg

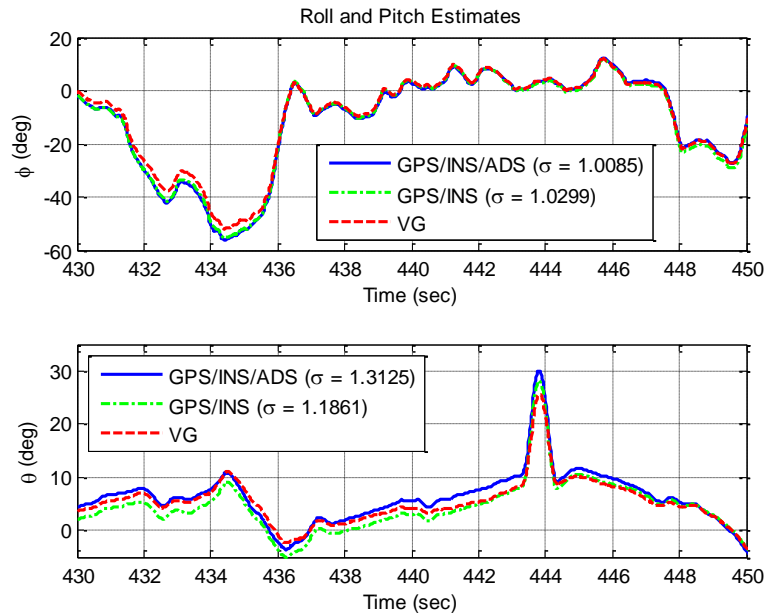


Fig. 4. Roll and Pitch Estimates with Vertical Gyroscope Reference

Although the flight data does not contain a ‘truth’ reference for the yaw angle, the components of velocity from GPS can be used to calculate the heading of the aircraft. The difference between the heading and yaw of the aircraft is the sideslip angle. A benefit of the GPS/INS/ADS formulation is the implicit estimation and regulation of the sideslip angle, β . This allows for distinct estimation of both the heading and yaw angles of the aircraft, which are assumed equal in standard GPS/INS attitude estimation. A 20 second segment of the estimated heading from yaw plus sideslip and calculated heading from GPS velocity is shown in Fig. 5. Close agreement is seen between these two calculations of heading. Additionally, the GPS/INS calculation of heading/yaw is shown in Fig. 5. It is clear that this approximation is not very good during this segment, as the sideslip oscillations are apparent in the signal. It is important to note that this comparison is for illustrative purposes only, as the GPS velocity is used in the calculation of yaw and sideslip, therefore the three calculations of heading are not independent.

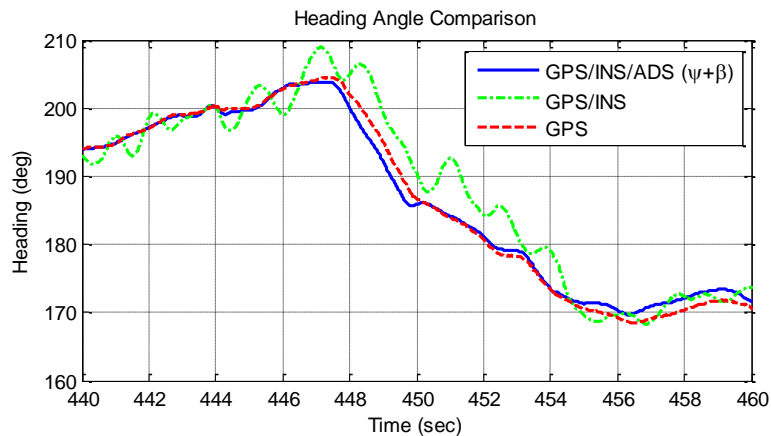


Fig. 5. Heading Angle Comparison

While it is possible to measure the angle of attack and sideslip angles of an aircraft through the use of wind vanes, these measurements contain various sources of uncertainty, including sensor noise, wind gust disturbances, and the inertial dynamics of the wind vane itself. Because of these uncertainties, the measurements of angle of attack and sideslip tend to be noisy. Calculating these angles from the body-axis velocity states leads to smoothed estimates. To illustrate this smoothing, a 10 second segment of the estimated angle of attack and sideslip angles are shown with the corresponding wind vane measurements in Fig. 6.

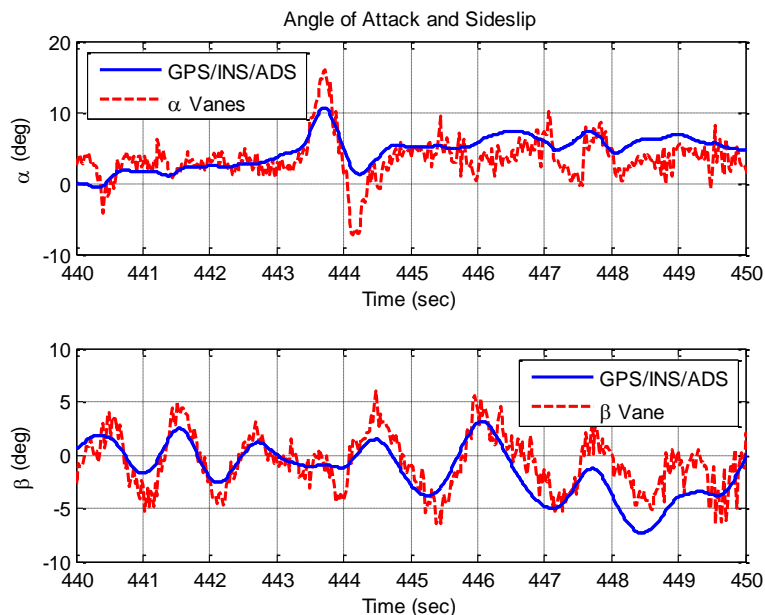


Fig. 6. Estimated and Measured Angle of Attack and Sideslip

It is shown in Fig. 6 that in addition to smoothing out the high frequency noise in the vane signals, the peaks tend to be less extreme in the GPS/INS/ADS estimate. This could partially be explained by the inertial properties of the physical vane itself, i.e. the vanes have mass, and under changes in aircraft trajectory, the vane's inertia will carry it beyond the actual airspeed direction before settling down to the appropriate value.

For comparison purposes, the total airspeed estimate from each formulation is compared with the ground speed from GPS as well as with the ADS measurement in Fig. 7.

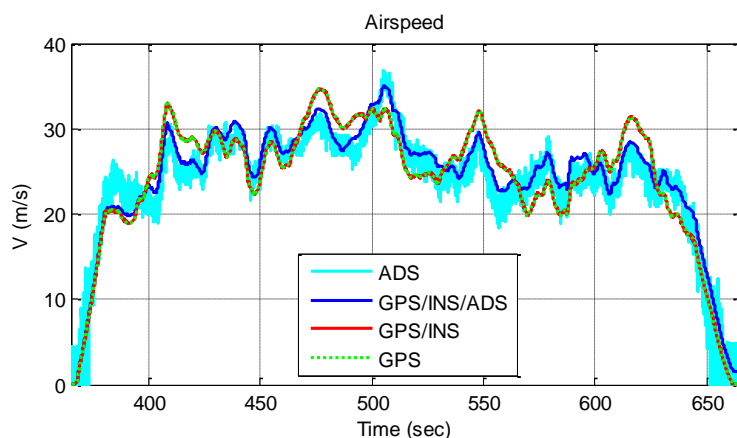


Fig. 7. Comparison of Airspeed, Ground Speed, and Pitot Tube Speed During Flight

It is shown in Fig. 7 that the GPS/INS/ADS formulation is able to obtain a much smoother estimate of the airspeed than is provided directly from the ADS. The GPS/INS formulation, however, estimates the airspeed as being approximately equivalent to the ground speed. The discrepancy in airspeed and ground speed is clearly demonstrated. This discrepancy occurs due to the local wind field, thus motivating the use of this formulation for wind estimation. The estimated wind components are given in Fig. 8.

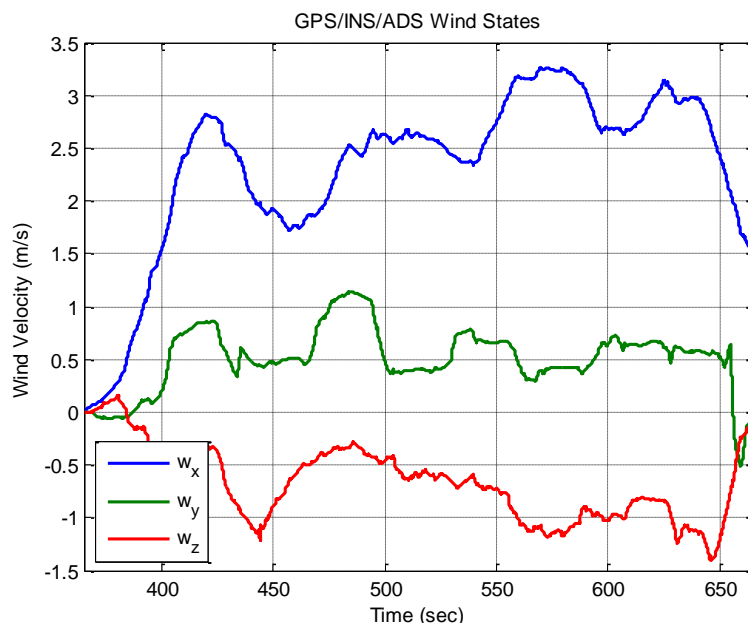


Fig. 8. Estimated Wind Velocity Components

In an effort to validate the wind estimation results, the horizontal planar wind speed and direction were calculated from the wind velocity component estimates and are plotted with the corresponding measurements from the ground weather station in Fig. 9. The wind speed reference from the weather station is shown in Fig. 9 with uncorrected measurements as well as measurements with the power law correction from (16).

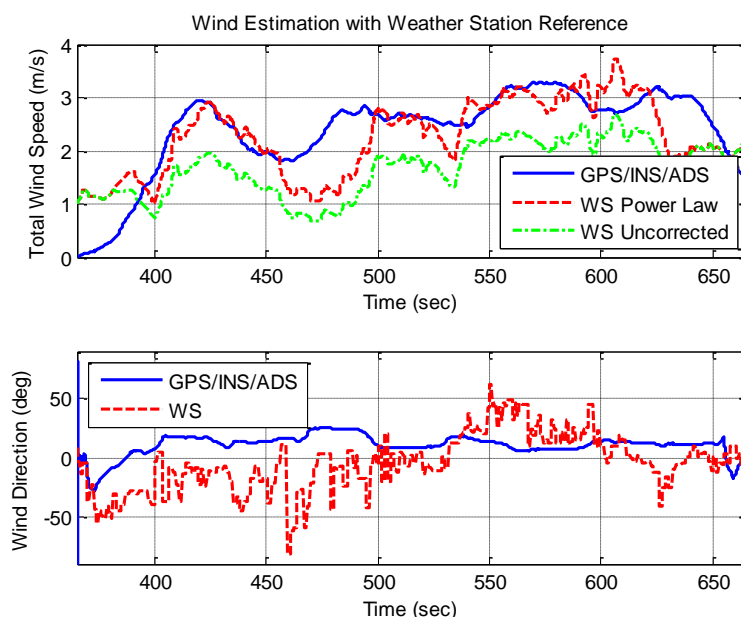


Fig. 9. Horizontal Planar Wind Speed and Direction

It is shown in Fig. 9 that the wind estimates are reasonable when compared with the ground weather station. These estimates do not closely match the ground weather station, which is to be expected since they are measuring different points in the local wind field, and local turbulence will cause changes in the measurement of the wind. Additionally, these measurements are compared at the same point in time, but due to the flow of the wind, this comparison is not truly valid. However, in general the wind estimates and ground weather station roughly agree,

which provides some justification that the wind estimation result is reasonable. In order to provide some statistical comparison, the GPS/INS/ADS estimates and weather station data can be used to calculate the wind field assuming it remains approximately constant in mean over the course of the flight. To obtain these values, the mean is taken over the period of flight. The results for the constant wind assumption are provided in Table 2. From these results it is clear that the power law correction is necessary for this application in order to more properly compare the wind speed. With this correction, the mean wind speed over the flight is very well approximated using the GPS/INS/ADS formulation. The constant wind direction estimation is not as good, with an error of approximately 16.7 degrees. A portion of this error is likely due to alignment errors when setting up the remote weather station. Also, this remote weather station has a course resolution of 6 degrees, which could partially contribute to the error.

Table 2. Constant Wind Field Estimation Results

	Mean Wind Speed	Mean Wind Direction
GPS/INS/ADS	2.27 m/s	9.54 deg
Wind Speed (Uncorrected)	1.67 m/s	-7.17 deg
Wind Speed (Power Law)	2.18 m/s	-7.17 deg

V. Conclusion

A new formulation of aircraft attitude estimation that incorporates air data system information was presented. A key distinction of this formulation compared to others is that the GPS velocity components are properly related to the body-axis velocity components through the consideration of wind. This effectively considers the wind triangle of airspeed, ground speed, and wind speed. Because of this adjustment, the estimated attitude states correspond to the actual orientation of the aircraft with respect to the fixed Earth. In particular, the yaw angle of the aircraft is able to be estimated independently of the heading angle through the consideration of sideslip. The experimental results demonstrated effective roll and pitch estimation performance, and the yaw estimate was reasonable when appropriately compared with GPS heading. A benefit of this formulation is that the estimated angle of attack and sideslip are smoother than the corresponding direct measurements from wind vanes, thus providing a means of filtering these measurements for use in other applications, such as parameter identification. Additionally, this formulation provided estimates of the wind speed and direction, which were validated with respect to a ground weather station.

Acknowledgments

This research was partially supported by NASA grant # NNX10AI14G and # NNX13AB74A. The authors would like to thank Francis J. Barchesky for developing the air data system avionics.

References

- ¹ Calise, A. J., and Rysdyk, R. T., "Nonlinear Adaptive Flight Control Using Neural Networks," *IEEE Control Systems*, Vol. 18, No. 6, Dec. 1999, pp. 14-25.
- ² Changchun, L., Li, S., Hai-bo, W., and Tianjie, L., "The research on unmanned aerial vehicle remote sensing and its applications," *Proc. of the IEEE International Conference on Advanced Computer Control (ICACC '10)*, Shenyang, China, March 2010, pp. 644-647.
- ³ Grewal, M. S., Weill, L. R., and Andrew, A. P., *Global Positioning, Inertial Navigation & Integration*, 2nd Ed., Wiley, New York, NY, USA, 2007.
- ⁴ Crassidis, J. L., "Sigma-point Kalman filtering for integrated GPS and inertial navigation," *Proc. of the AIAA Guidance, Navigation, and Control Conference and Exhibit*, San Francisco, CA, USA, 2005.
- ⁵ van der Merwe, R. D., Wan, E. A., and Julier, S. I., "Sigma-point Kalman filters for nonlinear estimation and sensor-fusion – applications to integrated navigation," *Proc. of the AIAA Guidance, Navigation, and Control Conference*, Providence, RI, USA, August 2004, pp. 1735-1764.
- ⁶ Fiorenzani, T., et al., "Comparative Study of Unscented Kalman Filter and Extended Kalman Filter for Position/Attitude Estimation in Unmanned Aerial Vehicles," *IASI-CNR*, R. 08-08, 2008.
- ⁷ Gross, J., Gu, Y., Rhudy, M., Gururajan, S., and Napolitano, M., "Flight test evaluation of GPS/INS sensor fusion algorithms for attitude estimation," *IEEE Trans. on Aerospace Electronic Systems*, Vol. 48, No. 3, July 2012, pp. 2128-2139.
- ⁸ Cho, A., Kim, J., Lee, S., and Kee, C., "Wind Estimation and Airspeed Calibration using a UAV with a Single-Antenna GPS Receiver and Pitot Tube," *IEEE Trans. on Aerospace and Electronic Systems*, Vol. 47, No. 1, Jan. 2011, pp. 109-117.
- ⁹ Kumon, M., Mizumoto, I., and Iwai, Z., "Wind Estimation by Unmanned Air Vehicle with Delta Wing," *Proc. of the 2005 IEEE International Conference on Robotics and Automation*, Barcelona, Spain, April 2005, pp. 1896-1901.
- ¹⁰ Langelaan, J. W., Alley, N., and Neidhoefer, J., "Wind Field Estimation for Small Unmanned Aerial Vehicles," *AIAA Guidance Navigation and Control Conference*, Toronto, Canada, 2010.

- ¹¹ Lefas, C. C., "Real-Time Wind Estimation and Tracking with Transponder Downlinked Airspeed and Heading Data," *IEEE Trans. on Aerospace and Electronic Systems*, Vol. AES-23, No. 2, March 1987, pp. 169-174.
- ¹² Kalman, R. E., and Bucy, R. S., "New Results in Linear Filtering and Prediction Theory," *Journal of Basic Engineering (Trans. of ASME)*, Vol. 83, 1961, pp. 95-108.
- ¹³ Klein, V., and Morelli, E. A., *Aircraft System Identification: Theory and Practice*, American Institute of Aeronautics and Astronautics, Inc., Reston, VA, 2006.
- ¹⁴ Roskam, J., *Airplane Flight Dynamics and Automatic Flight Controls*, DARcorporation, Lawrence, KS, USA, 2003.
- ¹⁵ Lewis, F. L., and Syrmos, V. L., *Optimal Control*, 2nd Ed., Wiley, NY, 1995.
- ¹⁶ Gross, J. N., Gu, Y., Rhudy, M., Barchesky, F. J., and Napolitano, M. R., "On-line Modeling and Calibration of Low-Cost Navigation Sensors," *AIAA Modeling and Simulation Technologies Conference*, Portland, OR, USA, Aug. 2011.
- ¹⁷ Allan, D. W., "Statistics of atomic frequency standards," *Proc. IEEE*, Issue 2, Vol. 54, Feb. 1966.
- ¹⁸ Xing, Z., Gebre-Egziabher, D., "Modeling and Bounding Low Cost Inertial Sensor Errors," *IEEE/ION Position, Location and Navigation Symposium*, Monterey, CA, USA, 2008, pp. 1122-1132.
- ¹⁹ Xing, Z., "Over-bounding Integrated INS/GNSS Output Errors," PhD Dissertation, The University of Minnesota, MN, USA, 2010.
- ²⁰ Julier, S., and Uhlmann, J., "A New Extension of the Kalman Filter to Nonlinear Systems," *SPIE Proceedings Series*, Vol. 3068, 1997, pp. 182-193.
- ²¹ Rhudy, M., Gu, Y., Gross, J., Gururajan, S., and Napolitano, M. R., "Sensitivity and Robustness Analysis of EKF and UKF Design Parameters for GPS/INS Sensor Fusion," *AIAA Journal of Aerospace Information Systems*, Vol. 10, No. 3, March 2013, pp. 131-143.
- ²² Rhudy, M., and Gu, Y., "Understanding Nonlinear Kalman Filters, Part I: Selection between EKF and UKF," *Interactive Robotics Letters*, West Virginia University, June 2013. Link: <http://www2.statler.wvu.edu/~irl/page13.html>.
- ²³ Rhudy, M., and Gu, Y., "Understanding Nonlinear Kalman Filters, Part II: An Implementation Guide," *Interactive Robotics Letters*, West Virginia University, June 2013. Link: <http://www2.statler.wvu.edu/~irl/page13.html>.
- ²⁴ Rhudy, M., Gu, Y., Gross, J., and Napolitano, M. R., "Evaluation of Matrix Square Root Operations for UKF within a UAV-Based GPS/INS Sensor Fusion Application," *International Journal of Navigation and Observation*, Vol. 2011, Article ID 416828, Dec. 2011.
- ²⁵ U.S. Environmental Protection Agency, "Meteorological Monitoring Guidance for Regulatory Modeling Applications," 2000.
- ²⁶ Elliott, D. L., "Adjustment and Analysis of Data for Regional Wind Energy Assessments," Workshop on Wind Climate, Asheville, North Carolina, November 12-13, 1979.